Chapter 4

Mechanical and Dynamic Mechanical Properties

The mechanical and dynamic mechanical properties of PP/HDPE blends as a function of blend ratio and compatibiliser concentration are discussed in this chapter. A detailed discussion on the fundamental reasons that are responsible for deterioration of properties in the absence and improvement in properties in the presence of compatibilisers is presented. The tensile strength of the uncompatibilised blends is theoretically modelled using Nielsen's and Nicolais-Narkis models. The Young's and storage moduli of uncompatibilised blends are compared with those predicted by various theoretical models. Attention is paid to correlate the mechanical properties of both compatibilised and uncompatibilised blends with their phase morphology.

A part of the results of this chapter has been published in European Polymer Journal, 40, 2105, 2004.

4.1. Introduction

Modern technology thrusts challenging demands on the performance capabilities of materials, including polymers and their blends. A new approach to the science and technology of polymer blends has emerged recently, i.e., polymer blends by design, rather than by availability [1]. These polymeric materials must perform under strenuous mechanical, chemical, thermal and electrical conditions imposed by the requirements of a specific application. Service in these applications usually involves several criteria to be fulfilled without a loss of economic advantage. Indeed, performance requirements of polymer blends are often at the limit of the properties that can be achieved. Moreover, these materials are expected to endure complex environmental conditions for extended time. Therefore the measurement of mechanical behaviour of the blends is of utmost importance.

The present chapter exclusively deals with the mechanical behaviour of polypropylene/high density polyethylene (PP/HDPE) blends. This involves both static and dynamic mechanical properties. Since the mechanical properties of polymer blends are affected to various degrees by the phase morphology, we tried to correlate the mechanical properties of the blends with their morphology with and without compatibilisers. The blends of PP and PE are commercially very important because of their high impact strength and low temperature toughness. Addition of PE into PP increases the impact strength of PP and addition of PP into PE improves the environmental stress crack resistance of PE. Hence these blends are technologically very important. Gohil [2] has found a synergism in mechanical properties through epitaxial growth in PE/PP blends. Spardaro and Rizzo [3] have observed that mixing parameters have significant effects on the mechanical properties and suggested that it is very important to find optimum mixing procedures for each kind of blends. Lee et al. [4] found that mechanical properties of PE/PP blends are closely related to the morphology.

Dynamic mechanical thermal analysis (DMTA) is another powerful technique to investigate the performance of polymer blends as it measures response of a material to cyclic stress. The investigation of dynamic modulus and damping behaviour over a wide range of temperatures and frequencies has proven to be

very useful in studying the structural features of polymer blends and the variation of properties with respect to end use applications [5,6]. These rely on structure, crystallinity, extent of cross-linking etc., which in turn depend on the phase morphology of the blends. Note that the dynamic mechanical properties are sensitive not only to different molecular motions but also to various transitions, relaxation processes, structural heterogeneity and the morphology of multiphase systems. Further, the dynamic mechanical properties of polymers give mirror image of their molecular and morphological features.

Another important aspect is that polymers are viscoelastic materials, which have some of the characteristics of both viscous liquids and elastic solids. Elastic materials have a capacity to store mechanical energy with no dissipation of energy; on the other hand, a viscous fluid in a non-hydrostatic stress state has a capacity for dissipating energy, but none for storing it. When polymeric materials are deformed, part of the energy is stored as potential energy and part is dissipated as heat. The energy dissipated as heat manifests itself as mechanical damping or internal friction. Therefore the interpretations of these properties at molecular level are of great scientific and practical importance in understanding the mechanical behaviour of the polymers.

Effects of blend ratio and compatibilisation on the mechanical and dynamic mechanical properties have been investigated by several researchers [7-18]. John et al. [14] have reported on the effect of blend ratio, dynamic vulcanisation and reactive compatibilisation on the dynamic mechanical properties of HDPE/EVA blends. They found that the presence of compatibiliser increased the storage and loss moduli and loss factor values of the system. The effect of different compatibilisers on the dynamic mechanical properties of PS/polybutadine blends was studied by Joseph [15]. The author reported that storage modulus, loss modulus and tanδ underwent dramatic changes in the presence of tri-block copolymers whereas no significant change has been observed in presence of random copolymers. Moly et al. [18] have studied the effect of compatibilisation on the dynamic mechanical properties of LLDPE/EVA blends and found that compatibilisation

increased the storage modulus of the system which is due to the fine dispersion of EVA domains in the LLDPE matrix providing an increased interfacial interaction.

As mentioned earlier, the main objective of this chapter is to investigate the effect of blend ratio and compatibiliser concentration on the mechanical and dynamic mechanical properties of PP/HDPE blends. In addition, we tried to compare the experimental data on tensile strength, Young's and storage moduli with theoretical models. Finally, attempts have been made to establish a correlation between the static and dynamic mechanical properties of the blends with and without compatibiliser and their morphology.

4.2. Results and discussion

4.2.1. Mechanical properties

4.2.1.1. Uncompatibilised blends

For incompatible blends containing at least one semi-crystalline component, the final tensile properties are determined by two competing factors: the increase in crystallinity due to the presence of more crystalline component and the extent of compatibility between the two component polymers. The former is the property determining factor at low strain level and the latter determines the properties at high strain level. The stress-strain behaviour of uncompatibilised PP/HDPE blends is demonstrated in Fig. 4.1. From the stress-strain curves, we estimated maximum tensile strength (σ_m), elongation at break (E_b) and Young's modulus (E).

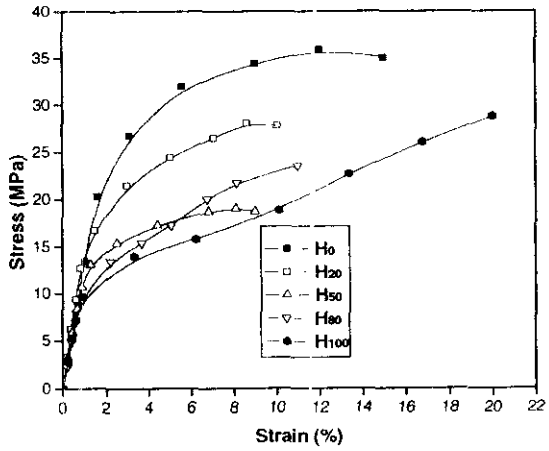

Figure 4.1: Stress-strain behaviour of uncompatibilised PP/HDPE blends

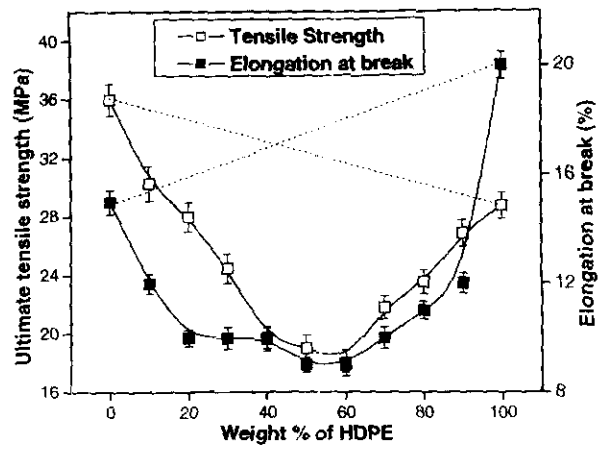

Figure 4.2: Effect of blend ratio on the ultimate tensile strength and elongation at break of uncompatibilised PP/HDPE blends

The σ_m and E_b values of uncompatibilised PP/HDPE blends are given in Fig. 4.2. It is seen from the figure that both these properties showed negative deviation from the additivity line indicating that the blends are highly incompatible. It is interesting to note that as the wt% of the minor phase increased the properties decreased and the minimum properties have been observed for blends containing 40-60wt% of one of the phases. This is in perfect correlation with the morphological parameters, which showed that as the wt% of the minor phase increased, the morphological stability decreased. This can be explained in terms of clustering phenomenon of the individual polymer during processing. Choi et al. [19] have reported that at temperatures above the crystallisation melting points of homopolymers, PE (132°C) and PP (165°C) chains are found to segregate into distinct domains and the PE phase shows more significant clustering. The clustering of PE and PP is due to the unfavourable cross-correlations between PE and PP chains in the blend [20]. This unfavourable clustering increases as the amount of individual polymer increases in the blend. Thus the incompatibility may be maximum for blends containing 40 to 60wt% of HDPE. Note that from the morphology studies, it has been found that this region is the co-continuous or semi co-continuous region.

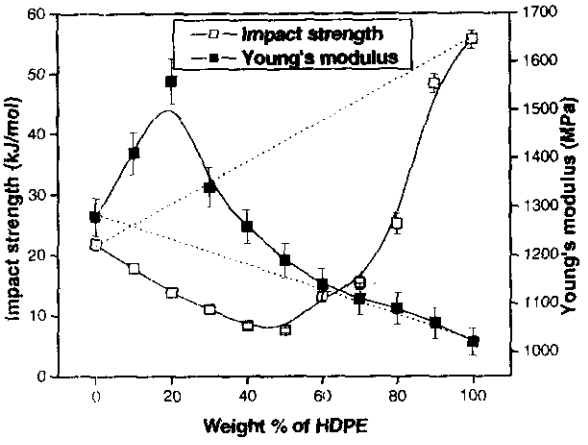

Figure 4.3: Effect of blend ratio on the impact strength and Young's modulus of uncompatibilised PP/HDPE blends

The impact toughness is often the deciding factor in material selection because impact test measures the ability of a polymer to withstand the load imposed upon being struck by an object at high velocity. Thus, it is a measure of the energy required to propagate a crack across the specimen. Therefore, the impact properties of these blends are especially important. The impact strength of HDPE is more than twice that of PP. From Fig. 4.3, it is obvious that the impact strength of blends also registered a negative deviation from the additivity line. However, it is seen that the impact properties are higher when HDPE forms the matrix due to the ductile nature of HDPE. On the other hand, as the wt% of one of the components increased, the impact strength decreased owing to the increased incompatibility with composition. As in the case of tensile strength and elongation values, impact strength also was minimum for blends with 40-60wt% of one of the phases.

Interestingly, it is found that Young's modulus experienced a synergism (Fig. 4.3). Note that compatibility of the blends does not play a major role in the case of Young's modulus since it is measured at low strain level. The synergism can be explained in terms of interfacial deformation of the blends. It is believed that during crystallisation of the matrix, deformation of the dispersed particles occurs and this

results in the deformation of the interface in polymer blends. Thus during the crystallisation of the blend where PP is the matrix phase, solidification of PP occurs in the presence of HDPE melt which constitutes the dispersed phase. During this process, molten HDPE flows into the region between PP spherulites growing near the interface. This results in the deformation of the interface between PP and HDPE, and the deformation ends with the completion of crystallisation of spherulites, when all the PP melt is converted to spherulites. The net result is an increase in interfacial area. For 90/10 blends (H_{10}) the HDPE concentration is too low to create deformation at the interfaces whereas for 70/30 (H_{30}) blends, the clustering of individual polymers is more pronounced than the deformation of the interface. Thus more stress transfer occurs in the case of 80/20 (H_{20}) blends. But unfortunately the formed interfaces are so weak that they can transfer stresses only at very low strain levels. This is why this blend shows synergism in Young's modulus, which is measured, at low strain levels. In short, all the properties except Young's modulus show negative deviation from additivity line and minimum values of mechanical properties are observed for blends exhibiting co-continuous morphology and these properties of the blends are intimately dependent on each and every change in the phase morphology.

4.2.1.2. Compatibilised blends

The effect of compatibilisation on the σ_m of H_{20} blends is given in Fig. 4.4. The σ_m of the blends increased by the incorporation of compatibilisers irrespective of the difference in their symmetry in terms of monomer fraction. This is in contrary to what observed from the morphology of the blends discussed in Chapter 3. However, it is also seen that the σ_m increased with increase in the amount of compatibiliser, reached maximum at 5wt% of the compatibiliser and beyond this almost levelling off in strength is observed. This is in good agreement with morphology of the blends, which revealed that 5wt% compatibiliser concentration was the interfacial saturation point (CMC) beyond which no effective compatibilisation took place.

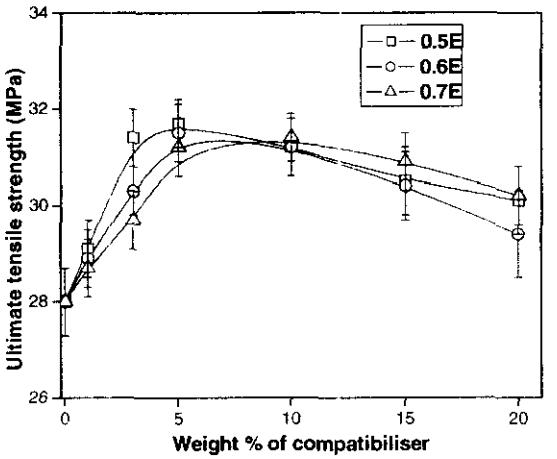

Figure 4.4: Effect of compatibilisation on the tensile strength of H_{20} blends

On the other hand, Fig. 4.5, which displays the effect of compatibilisers on the E_b of the blends, revealed that E_b increased with compatibiliser concentration. Even though there is no true levelling off in elongation, the rate of increase decreased beyond 5wt% of the compatibiliser concentration. Further, unlike tensile properties, there is difference in performance of different compatibilisers. As morphological studies illustrated, 0.5E was found to be most effective. Thus E_b values can be correlated with the morphology of the blends.

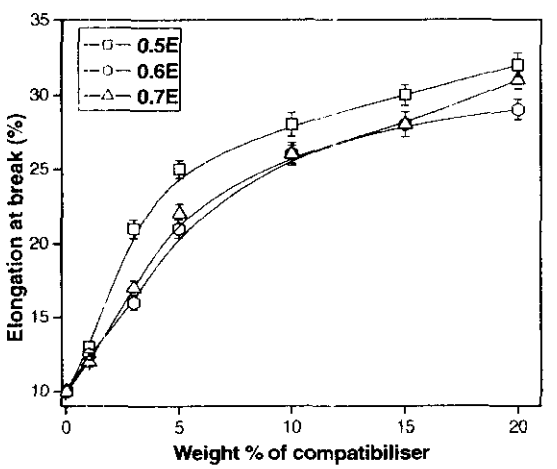

Figure 4.5: Effect of compatibilisation on the elongation at break of H_{20} blends

The Young's modulus presented in Fig. 4.6, on the other hand, shows a different behaviour. As the compatibiliser concentration increased, the Young's modulus experienced marginal decrease. This is basically due to the combined effects of two phenomena. First, since Young's modulus is measured at low strain level, as mentioned earlier, compatibility has no significant role. The presence of compatibiliser, indeed increased the compatibility and therefore enhanced most of the mechanical properties of the blends, but does not have an impact on the Young's modulus. Thus increase in compatibility does not increase the Young's modulus. Now, why the Young's modulus registered lower values in the presence of compatibiliser? There are two possibilities: (i) the addition of compatibiliser may reduce the crystallinity of the individual polymer and thereby decrease the Young's modulus. This can be ruled out by the fact that we observed that compatibilisers have no significant effect in the crystallisation behaviour of PP and HDPE (will be discussed in Chapter 5) and (ii) the compatibilisers may increase the softness of the blends and thus decrease the Young's modulus. Since the compatibiliser is a flexible polymer, this is a more probable reason for the decrease in Young's modulus.

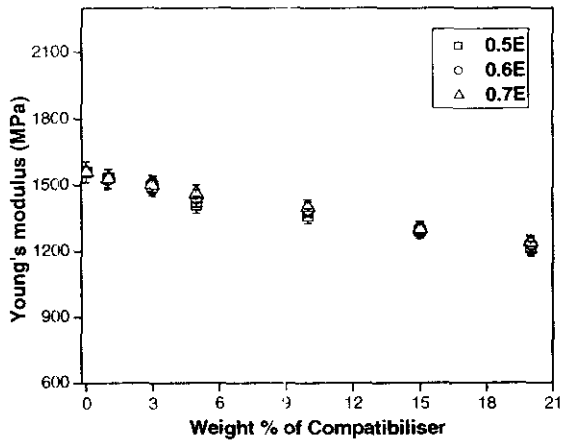

Figure 4.6: Effect of compatibilisation on the Young's modulus of H_{20} blends

Effect of compatibilisers on the impact strength of the blends is demonstrated in Fig. 4.7. There is remarkable difference in the compatibilising efficiency of random copolymers in terms of impact strength. 0.5E was found to the best compatibiliser.

The impact strength becomes almost twice in presence of even 5wt% of 0.5E. Other compatibilisers also enhanced the impact strength, but to a lesser extent compared to the symmetric compatibiliser. Thus it is the impact strength, which showed maximum correlation with morphology in terms of the compatibilising efficiency. However, like E_b, impact strength also experienced no levelling off at 5wt%, but the rate of increase in property decreased beyond this limit. In short all the mechanical properties except the Young's modulus improved in the presence of compatibilisers and there is very good link between the mechanical properties and phase morphology of the blends in the presence of compatibilisers.

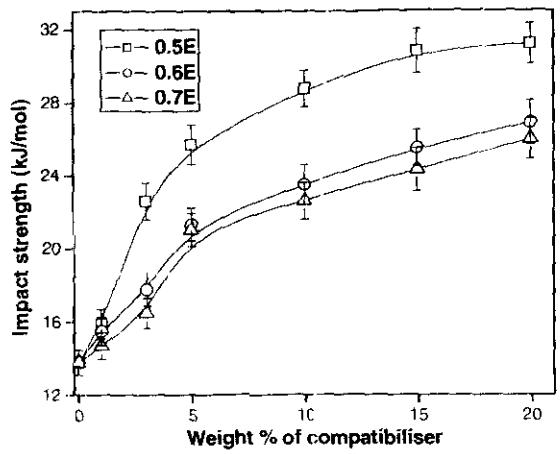

Figure 4.7: Effect of compatibilisation on the impact strength of H_{20} blends

4.2.1.3. Theoretical modeling

4.2.1.3.1. Theoretical analysis of tensile strength

In order to understand the level of interaction between the component polymers in PP/HDPE blends, predictive models were used to tensile strength data. These models include:

i. Nielsen's first power law model [21]: $\frac{\sigma_b}{\sigma_p} = (1-\phi_1)S$ (4.1)

ii. Nielsen's two-third power law model [21]: $\frac{\sigma_b}{\sigma_p} = \left(1-\phi_1^{2/3}\right)S$ (4.2)

iii. Nicolais-Narkis model [22]: $\frac{\sigma_b}{\sigma_p} = \left(1-K_1\phi_1^{2/3}\right)$ (4.3)

where σ_b and σ_p represent the tensile strength of the blend and the major component of the blend, respectively, ϕ_1 is the volume fraction of the minor phase, S and S' are Nielsen's parameters in the first and two-third power law models respectively and K_b is an adhesion parameter. S and S' account for the weakness in the structure brought about by the discontinuity in stress transfer and generation of the stress concentration at the interfaces in the case of blends. The values of S and S' are unity in the case of no stress concentration effect. The value of K_b is 1.21 for spherical inclusions of the minor phase having no adhesions. The values of relative tensile strength (σ_b/σ_p), S, S' and K_b are listed in Tables 4.1 and 4.2. Plots of relative tensile strength versus volume fraction of the blends predicted using the three models are presented in Figs. 4.8 and 4.9.

Blend	σ_b/σ_p	S	S'	K_b
H_{10}	0.85	0.94	1.07	0.74
H_{20}	0.78	0.95	1.15	0.69
H_{30}	0.68	0.94	1.18	0.75
H_{40}	0.54	0.86	1.12	0.89
H_{50}	0.53	0.99	1.32	0.79
Mean	0.675	0.936	1.167	0.773

Table 4.1: Relative tensile strength and adhesion parameters of PP rich blends

Blend	σ_b/σ_p	S	S'	K_b
H_{90}	0.93	1.03	1.18	0.32
H_{80}	0.82	1.01	1.22	0.55
H_{70}	0.70	1.06	1.33	0.56
H_{60}	0.63	1	1.30	0.72
H_{50}	0.66	1.24	1.65	0.56
Mean	0.75	1.07	1.34	0.54

Table 4.2: Relative tensile strength and adhesion parameters of HDPE rich blends

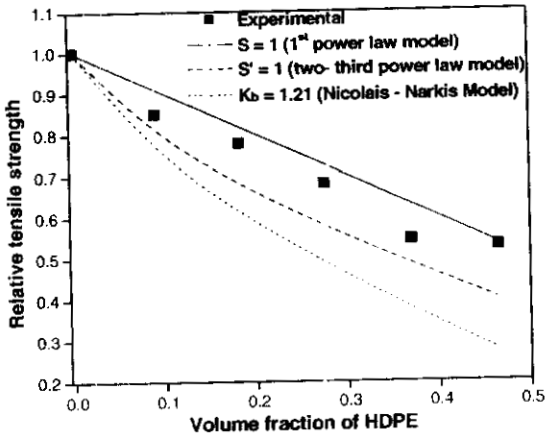

Figure 4.8: Plot of relative tensile strength versus volume fraction of dispersed HDPE phase using different models

From Fig. 4.8, it is obvious that in all the blends the experimental data are far away from that predicted by the models (expect for 50/50 blends which is very close the value predicted by Nielsen's first power law model). It should be noted that the curves predicted by the models are based on the perfect adhesion conditions and the deviation clearly shows that all the blends are incompatible with no adhesion between components. In this point of view, it can be stated that all the models are in good agreement with the experimental data when PP forms the major phase.

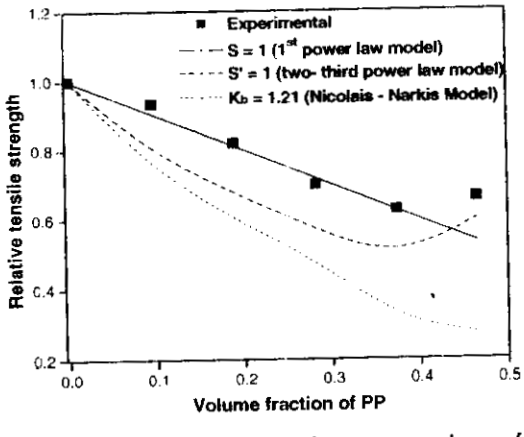

Figure 4.9: Plot of relative tensile strength versus volume fraction of dispersed PP phase using different models

On the other hand, Fig. 4.9 shows that in the case of HDPE rich blends the experimental data are in perfect agreement with that predicted by Nielsen's first power law model except for H_{50} blends (note that H_{50} has a co-continuous phase structure). This means that when HDPE forms the matrix the first power law model suggested that there is perfect adhesion between the two components in the blend. But this is not true in terms of morphology (Chapter 3) and mechanical properties. Thus experimental data are not in agreement with first power model. On the other hand, other two models suggest that there is no adhesion between the components.

4.2.1.3.2. Theoretical analysis of Young's modulus

In order to understand the behaviour of Young's modulus, applicability of various composite models such as parallel, series, Coran and Takayanagi models is examined. The upper bound parallel model is given by the rule of mixtures as follows [23]:

$$E_u = \phi_1 E_1 + \phi_2 E_2 \tag{4.4}$$

This model is applicable to the materials in which the components are connected parallel to one another so that the applied stress lengthens each component to the same extent. In the lower bound series model, the blend components are arranged in series (Reuss prediction) perpendicular to the direction of the applied force. The modulus prediction is given by the inverse rule of mixtures as:

$$\frac{1}{E_L} = \frac{\phi_1}{E_1} + \frac{\phi_2}{E_2} \tag{4.5}$$

In these models E_u is the modulus of the blend in the upper bound parallel model and E_L the modulus of the blend in the series model. E_1 and E_2 are the mechanical properties of components 1 and 2, respectively; ϕ_1 and ϕ_2 are their corresponding volume fractions. For both these models, no morphology is required, but strain or stress can be continuous across the interface, and Poisson's ratio is the same for both phases.

According to Coran's equation [24]

$$M = f(M_U - M_L) + M_L \tag{4.6}$$

where f can vary between zero and unity. The value of f is given by

$$f = V^n{}_H \left(nV_S + 1\right) \tag{4.7}$$

where n contains the aspects of phase morphology, and V_H and V_S are the volume fractions of the hard phase and soft phase respectively.

Takayanagi proposed a series-parallel model [25,26] in which, the concept of percolation is introduced. It is a phenomenological model consisting of mixing rule between two simple models involving connection in series (Reuss prediction) or in parallel (Voigt prediction) of the components. According to this model,

$$E = (1-\lambda)E_1 + \lambda\left[(1-\phi)/E_1 + (\phi/E_2)\right]^{-1} \tag{4.8}$$

E_1 is the property of the matrix phase, E_2 is the property of the dispersed phase, and ϕ is the volume fraction of the dispersed phase and is related to the degree of series-parallel coupling. The degree of parallel coupling of the model can be expressed by

$$\% \text{ parallel} = [\phi\ (1-\lambda) / (1-\phi\ \lambda)] \times 100 \tag{4.9}$$

From Fig. 4.10, which compares the experimental data and the predictive models, it is seen that when PP forms the matrix, (up to 60wt% of PP), none of the model is in agreement with the experimental data. On the other hand, when PP forms the dispersed phase, the experimental data are in agreement with all the models. It is plainly clear that the difference in behaviour before and after the phase inversion is due to the synergism exhibited by the blends when PP forms the matrix, especially at 80wt% PP. The synergism was explained on the basis of the deformation of the spherulites and none of the models considers this aspect.

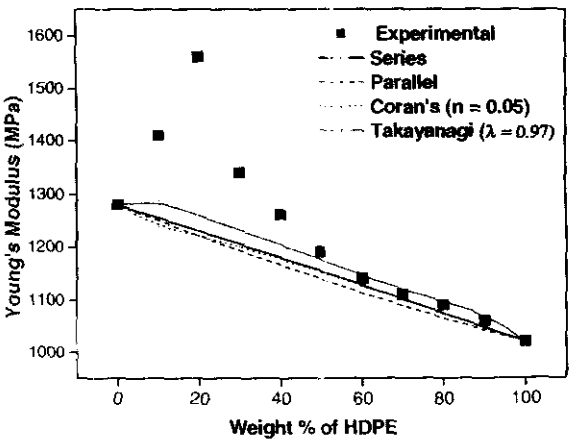

Figure 4.10: Plots of experimental and theoretical Young's moduli as a function of wt% of HDPE

4.2.2. Dynamic mechanical properties

4.2.2.1. Uncompatibilised blends

As mentioned earlier, dynamic mechanical thermal analysis helps to measure the glass transition temperature (T_g) of polymers. In addition one can obtain an idea about the storage (dynamic) modulus, loss modulus and damping behaviour (internal friction). T_g of polymers is a very important parameter since there are profound changes in the physical properties of polymers such as heat capacity, thermal expansion coefficient and modulus occur at this temperature. The modulus indicates stiffness of material and the mechanical damping gives the amount of energy dissipated as heat during the deformation. Further, it should be noted that T_g of polymers is accompanied by a sharp decrease in stiffness. The stress relaxation modulus decreases and the creep compliance increases by about three orders of magnitude in glass transition region. The loss moduli and loss compliances exhibit a maximum in the glass transition region as does tan δ. Any type of interaction between the polymers will give rise to a shift in this maximum and thus dynamic mechanical measurements will provide an idea about the extent of interactions between the component polymers in a polymer blend.

Generally, high molecular weight polymers, due to their viscoelastic nature display different types of behaviour viz. glassy, viscoelastic, rubbery and viscous liquid

behaviour, depending on temperature. At very low temperature, polymers are in glassy state at which they are hard and elastic. In this temperature range, the thermal energy is insufficient to surmount the potential energy barriers for rotational and translational motions of segments of the polymer molecules. The chain segments are essentially frozen in fixed positions as they can have only vibrational motions around fixed positions. With increase in temperature, the amplitude of vibrational motion becomes greater, and eventually, the thermal energy becomes comparable to the potential energy barrier for the segment rotation. In this temperature range where short-range diffusional motions of chain segments begin, the polymer is said to be at the glass transition temperature (T_g). The polymer in this region exhibits leathery behaviour. As the temperature is further increased, the short range segmental motions that initially gave rise to the glass transition occur very much faster but the long range cooperative motion of chain segments that would result in translational motions of complete molecules is still restricted by the presence of chain entanglements which act as temporary cross links. In this temperature region, called rubbery state, segments of chains reorient relative to each other but large scale translational motions do not occur. A further increase of temperature causes molecular motions to increase until complete polymer chains begin to translate relative to one another and this results in molecular flow; the polymer then become a viscous liquid. The corresponding temperature interval is called the flow region.

Figure 4.11 demonstrates the effect of blend ratio on the storage modulus (E') of PP/HDPE blends. PP exhibits the maximum and HDPE the minimum storage moduli in the whole temperature range. The E' of all the blends exhibit intermediate values. As the wt% of HDPE in the blend increases, storage modulus decreases even though there is some discrepancy at temperatures above 70°C. However, it is interesting to compare the Young's modulus with storage modulus since both are measured under tension (Fig. 4.12). One can expect similar values and trend for both. However the E' values offer apparent conflict with the Young's moduli and are considerably higher than the Young's moduli. At the same time there is no synergism in the E' values.

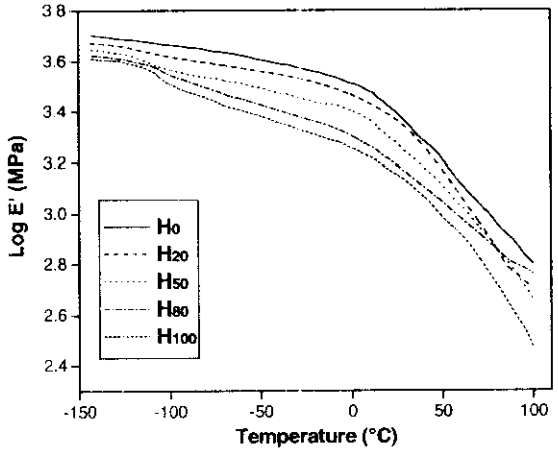

Figure 4.11: The variation of storage modulus of PP, HDPE and their blends as a function of temperature.

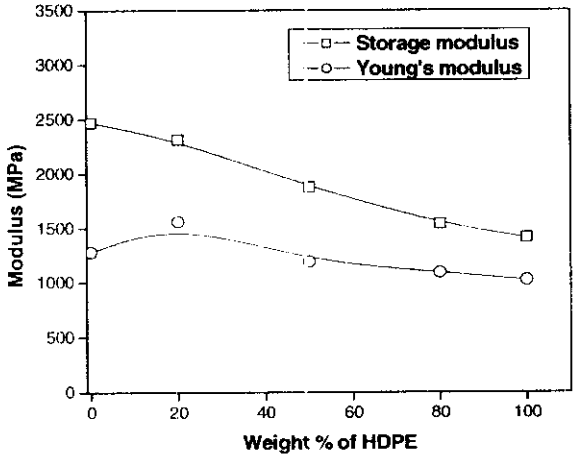

Figure 4.12: Comparison of the moduli values obtained from dynamic mechanical and static mechanical tests.

The effect of blend ratio on the T_g's of PP and HDPE obtained from the loss modulus (Fig. 4.13) and tan δ (Fig. 4.14) curves is given in Table 4.3. From the figures, it is seen that the T_g of HDPE and PP are ca. –120 and 10°C, respectively. The blend ratio has no impact on the T_g of individual polymer indicating that blends are highly immiscible and incompatible.

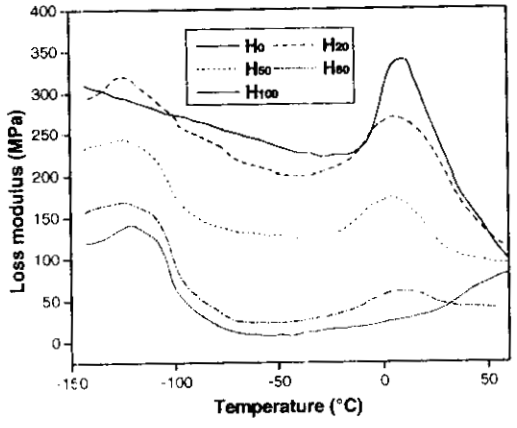

Figure 4.13: Effect of blend ratio on the variation of loss modulus as a function of temperature

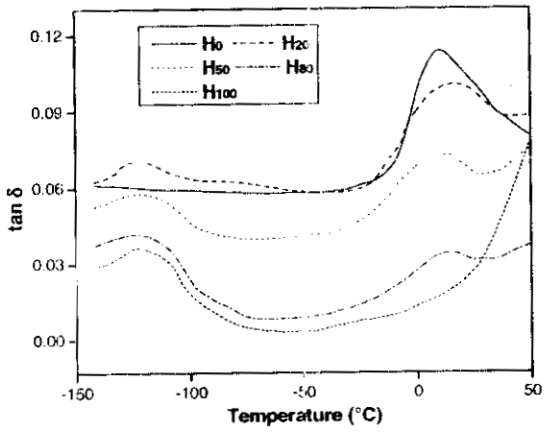

Figure 4.14: Effect of blend ratio on the variation of tan δ as a function of temperature

System	From loss modulus		From tan δ	
	HDPE Phase	PP Phase	HDPE Phase	PP Phase
H_0	---	10	---	8
H_{20}	-122	10	-124	7
H_{50}	-120	10	-123	6
H_{80}	-121	13	-122	7
H_{100}	-122	--	-120	-

Table 4.3: Effect of blend ratio on the glass transition temperatures of PP and HDPE

4.2.2.2. Theoretical analysis of storage modulus

Figures 4.15-4.17 present the comparison of experimental and theoretical values of storage modulus of PP/HDPE blends in the whole temperature range. First, consider H_{20} blends (Fig. 4.15): It is seen that the experimental results are in good agreement with all theoretical models except Takayanagi model which is in agreement with the experimental curve only in a limited temperature range (20-50°C). Note that the best fit was obtained with 20% parallel coupling in Takayanagi model that is equal to the wt% of the dispersed HDPE phase which is assumed to be the soft segment in the blend.

Secondly, consider H_{80} blends (Fig. 4.16): Note that experimental data are in agreement with all the models including Takayanagi model up to ~40°C beyond this temperature the experimental curve moves away from the different models. It should be noted that in the case of Takayanagi model, best fit is obtained with 80% parallel coupling which is equal to the weight percentage of HDPE, which is the matrix.

Finally, for H_{50} blends (Fig. 4.17), it is seen that experimental curves are in good agreement with all predictive models except Takayanagi model in the whole temperature range. Interestingly, the curve predicted by Takayanagi model is well above the experimental curve. Note that the best fit is obtained with 50% parallel coupling. Thus in short, in the case of all the blends, experimental data are in agreement with the theoretical models except Takayanagi model. However, it is important to note that the best fit curve is obtained in the case of Coran's model when the 'n' values are very low; n= 0.15, 0.004 and 0.018 for H_{20}, H_{80} and H_{50} blends, respectively ('n' is a parameter related to the phase morphology of the blends). This is usually unlikely and the values of 'n' will be greater than 1 [24]. The exceptionally low value of 'n' can be explained by taking in to account of the fact that Coran's model was originally proposed for thermoplastic elastomers with a hard matrix and an elastomeric minor phase. However, in the present case, the minor phase is not elastomeric and there is no distinction between the nature of two phases, consequently 'n' values are very low.

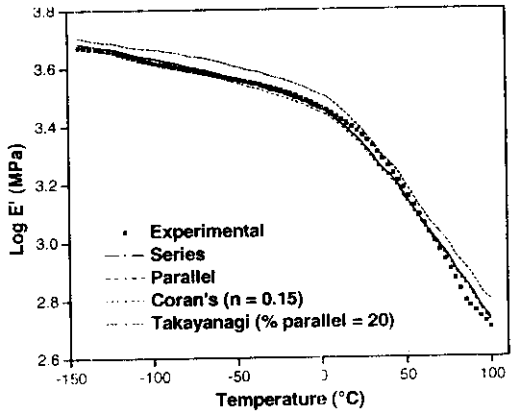

Figure 4.15: Experimental and theoretical curves of storage modulus of H_{20} blends in the whole temperature range

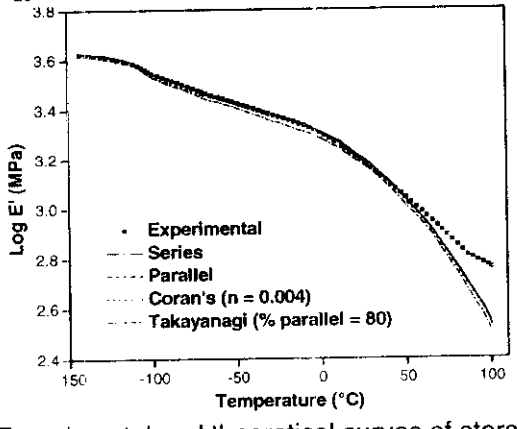

Figure 4.16: Experimental and theoretical curves of storage modulus of H_{80} blends in the whole temperature range

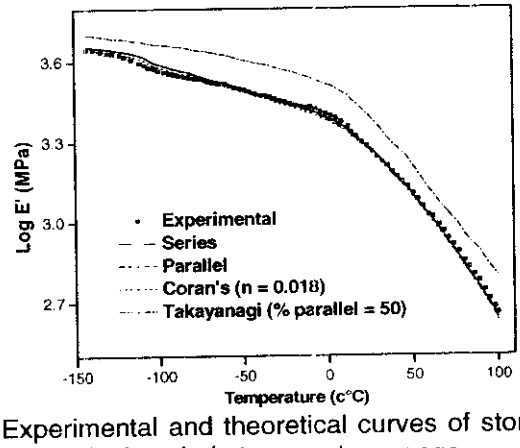

Figure 4.17: Experimental and theoretical curves of storage modulus of H_{50} blends in the whole temperature range

We have also estimated the effect of blend ratio on the experimental and theoretical storage moduli of PP/HDPE blends at three selected temperatures (see Figs. 4.18-4.20). The selected temperatures are the T_g's of PP (~10°C) and HDPE (~-120°C) and room temperature. It is obvious from the figures that all the blends show similar behaviour at these temperatures. Further, it is seen that Takayanagi model shows deviation in all the cases. In addition, all the curves except the one corresponding to Takayanagi model are very close to each other mainly due to the fact that there is no big difference between the storage moduli of PP and HDPE.

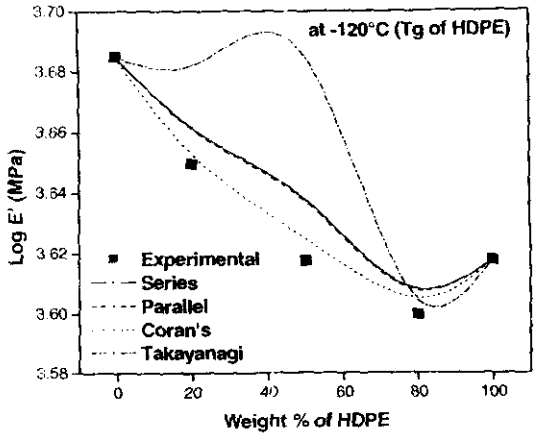

Figure 4.18: Comparison of the experimental and theoretical data of storage modulus of PP/HDPE blends at the T_g of HDPE

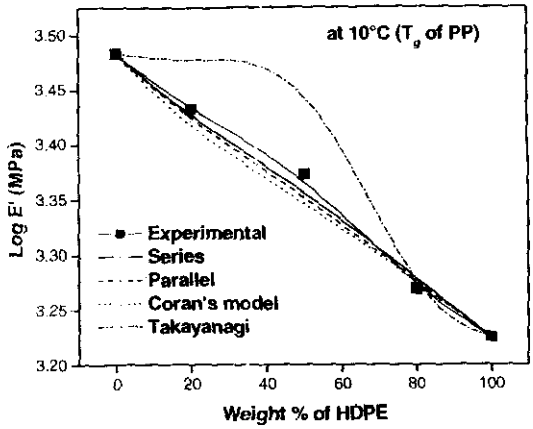

Figure 4.19: Comparison of the experimental and theoretical data of storage modulus of PP/HDPE blends at the T_g of PP

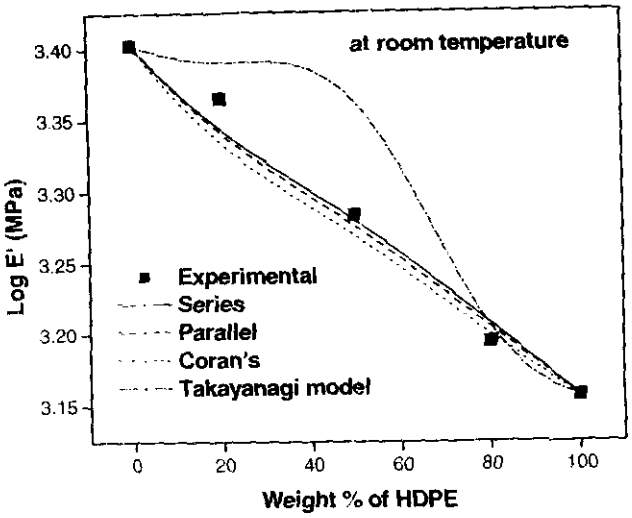

Figure 4.20: Comparison of the experimental and theoretical data of storage modulus of PP/HDPE blends at room temperature

4.3. Conclusions

The mechanical and dynamic mechanical properties of PP/HDPE blends with and without compatibilisers have been extensively studied in this chapter. The uncompatibilised PP/HDPE blends exhibit inferior mechanical properties (except for Young's modulus) due to the lack of interfacial interactions between the phases. The Young's modulus showed synergism and maximum property was obtained for 80/20 PP/HDPE (H_{20}) blends. The synergism was explained on the basis of the interfacial deformation of the blends since solidification of PP occurs in the presence of HDPE melt which constitutes the dispersed phase in H_{20} blends. During this process, molten HDPE flows into the region between PP spherulites growing near the interface that results in the deformation of the interface between PP and HDPE which in turn results in an increase in interfacial area. For 90/10 blends the HDPE concentration is too low to create deformation at the interfaces whereas for 70/30 blends, the clustering of individual polymers is more pronounced than the deformation of the interface. Thus more stress transfer occurs in the case of 80/20 blends. Compatibilisers improved the mechanical properties of the blends (except Young's modulus) extensively. The symmetric compatibiliser was most efficient. Even though the increase in tensile strength was

only marginal (~<15%), the elongation at break (~150%) and impact strength ((~90%) enhanced substantially. The mechanical properties of the blends in the presence of compatibilisers could be correlated with the phase morphology.

Dynamic mechanical properties of the blends showed that the glass transition temperature of HDPE and PP are ca. −120 and 10°C. Blending has little impact on the T_g's of the individual polymer due to the immiscible and incompatible nature of the blends. PP possessed maximum storage modulus, HDPE the minimum and all the blends exhibited intermediate values. Unlike Young's modulus, storage modulus didn't pass through a maximum indicating no synergism. Compatibiliser shifted the T_g's of the individual polymer towards each other indicating better compatibility in the presence of compatibiliser.

The experimental tensile strength of uncompatibilised blends was compared with predictive models such as Nielsen's first and two-third power law models and Nicolais-Narkis model. It was found that when PP formed the matrix, all the models offer good agreement with the experiment. On the other hand, when HDPE formed the matrix, the first power law model deviated from the experimental data. The experimental Young's modulus was compared with a series of models such as Parallel, Series, Coran's and Takayanagi models and found that none of the models could provide reasonable agreement with the experimental data when PP formed the matrix due to the synergism shown by the blends. The experimental storage modulus was compared with different predictive models and found that blends with dispersed phase morphology offered reasonable agreement with all the models whereas that with co-continuous phase morphology showed agreement with all the models except Takanyagi model in the whole temperature range.

4.4. References

1. L.A. Utracki, Introduction to Polymer Blends, in Polymer Blends Handbook, L.A. Utracki, Ed., Volume 1, Kluwer Academic Publishers, Dordrecht, (2002)

2. R.M. Gohil, J. Polym. Sci. Polym. Phys. Ed., **23**, 1713, 1985.

3. G. Spardaro, G. Rizzo, Eur. Polym. J., **25**, 1189, 1989.

4. Y.K. Lee, Y.T. Jeong, K.C. Kim, H.M. Jeong, B.K. Kim, Polym. Eng. Sci., **31**, 944, 1991.

5. T. Murayama, in Dynamic Mechanical Analysis of Polymeric Materials, Ch. 3, *Elsevier Scientific, New York, (1978).*

6. L.E. Nielsen, in Mechanical Properties of Polymers, Van Nostrand Reinhold, New York, (1962).

7. B. Kuriakose, S.K. De, S.S. Bhagawan, R. Sivaramkrishnan, S.K. Athithan, J. Appl. Polym. Sci., **32**, 5509, 1986.

8. T. Karger Kocsis, L. Kiss, Polym. Eng. Sci., **27**, 254, 1987.

9. H. Varghese, S.S. Bhagavan, S.S. Rao, S. Thomas, Eur. Polym. J., **31**, 957, 1995.

10. B. Brahimi, A. Ait-Kadi, A. Ajji, R. Fayt, J. Polym. Sci. B: Polym. Phys., **29**, 946, 1991.

11. J. George, K.T. Varughese, S. Thomas, Polymer, **41**, 1507, 2000.

12. T.Y. Guo, M.D. Song, G.J. Hao, B.H. Zang, Eur. Polym. J., **37**, 241, 2001.

13. S.C. Tjong, R.H. Yang, M. Lai, W. Lin, C. Sun, J. Lin, J. Appl. Polym. Sci., **85**, 2600, 2002.

14. *B. John, K.T. Varughese, Z. Oommen, S. Thomas, J. Appl. Polym. Sci.,* **87**, 2083, 2003.

15. S. Joseph, Ph. D thesis, Mahatma Gandhi University, 2004.

16. E.R. Vargas, Z.S. Arellano, J.S.H. Valdez, J.G.M. Colunga, S.S. Valdes, J. Appl. Polym. Sci., **100**, 3696, 2006.

17. M.F. Diaz, S.E. Barbosa, N.J. Capiati, Polym. Eng. Sci., **46**, 329, 2006.

18. K.A. Moly, S.S. Bhagawan, G. Groeninckx, S. Thomas, J. Appl. Polym. Sci., **100**, 4526, 2006.

19. P. Choi, H.P. Blom, T.A. Kavassalis, A. Rudin, Macromolecules, **28**, 8247, 1995.

20. J.J. Rajasekaran, J.G. Curro, J.D. Heneycutt, Macromolecules, **28**, 6843, 1995.

21. L.E. Nielsen, J. Appl. Polym. Sci., **10**, 97, 1966.

22. L. Nicolais, M. Narkis, Polym. Eng. Sci., **11**, 194, 1971.

23. J. George, Ph.D Thesis, Mahatma Gandhi University, 2004.

24. A.Y. Coran, Handbook of Elastomers, New developments and Technology, Eds. A.K. Bhownick, H.L. Stephens, Marcel Dekker, New York, (1988).

25. R.A. Dickie, J. Appl. Polym. Sci., **17**, 45, 1973.

26. R.M. Holsto-Miettiner, J.Y. Seppala, O.T. Ikkala, I.T. Reima, Polym. Eng. Sci., **34**, 395 1994.